Electronic Supplementary Material (ESI) for Environmental Science: Processes & Impacts.

Supporting Information

Abiotic reduction of nitrite by Fe(II): A comparison of rates and N_2O production

Thomas Robinson,[†] Drew E. Latta,[†] Luiza Notini,[†] Keith E. Schilling,[‡] and Michelle M. Scherer[†]

†Department of Civil and Environmental Engineering, University of Iowa, Iowa City, Iowa 52242, United States

‡Iowa Geological Survey, 300 Trowbridge Hall, Iowa City, IA 52242-1319,
United States

Figures: 6

Tables: 2

Pages: 16

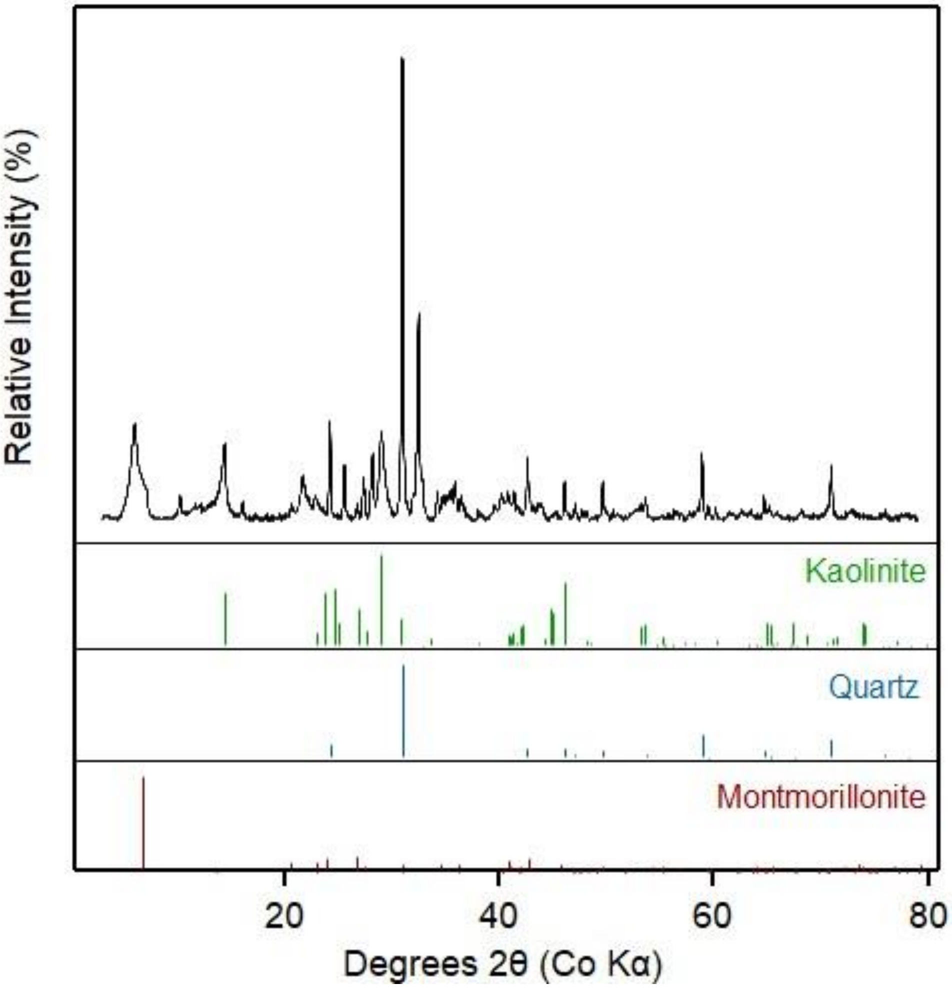

Figure S1. X-Ray diffraction pattern of Walnut Creek sediment.

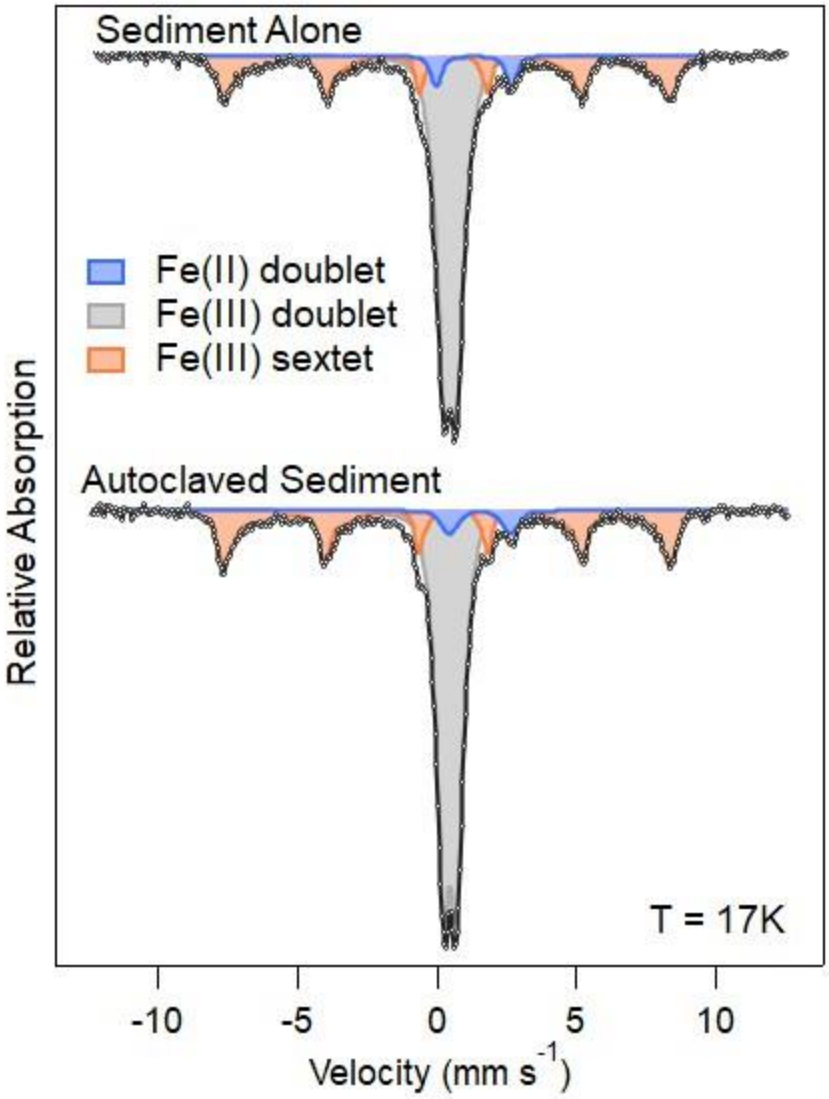

Figure S2. ^{57}Fe Mössbauer spectra of Walnut Creek sediment before (top), and after (bottom) autoclaving. Open circles represent data points and lines connect adjacent data points for a visual aid.

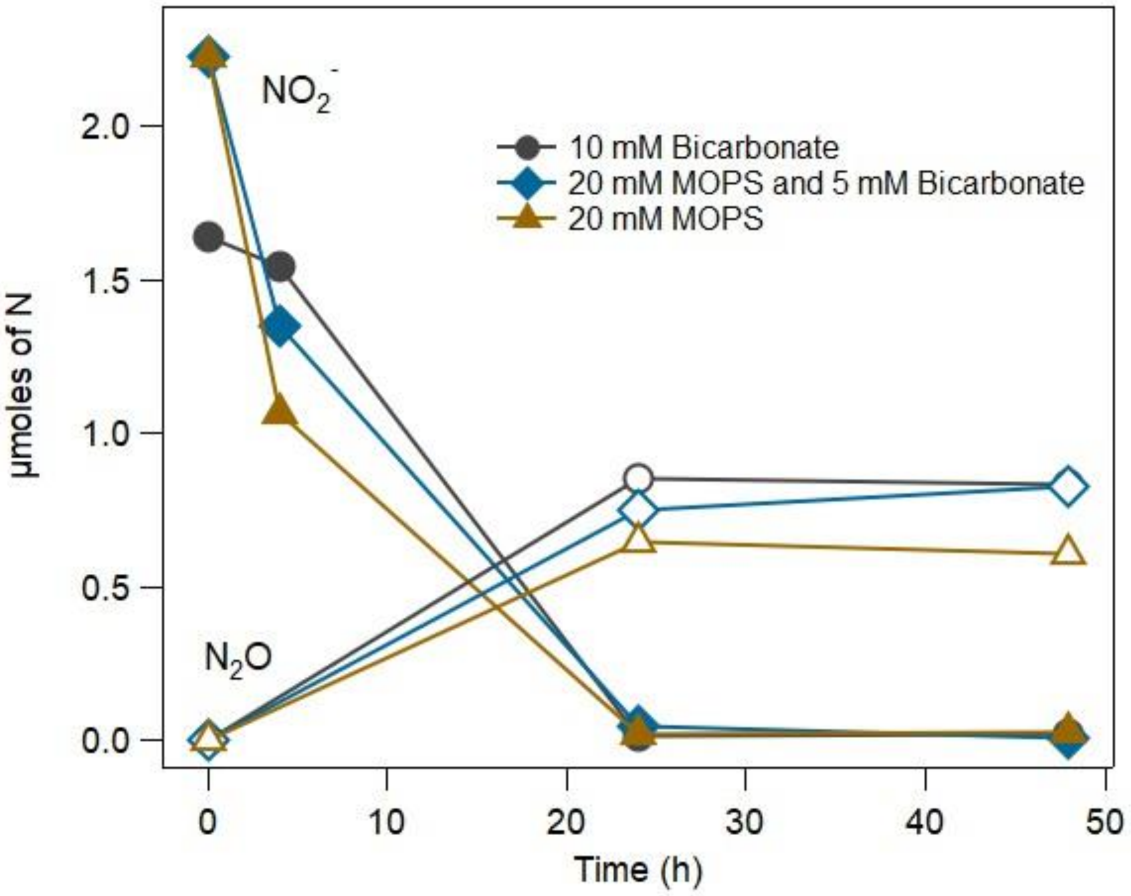

Figure S3. Nitrite reduction and nitrous oxide production by hematite and Fe(II) in the presence of different buffers. **Experimental conditions:** 5 g/L Hematite, 1 mM Fe(II), 0.1 mM NO_2^-, initial pH 7.0

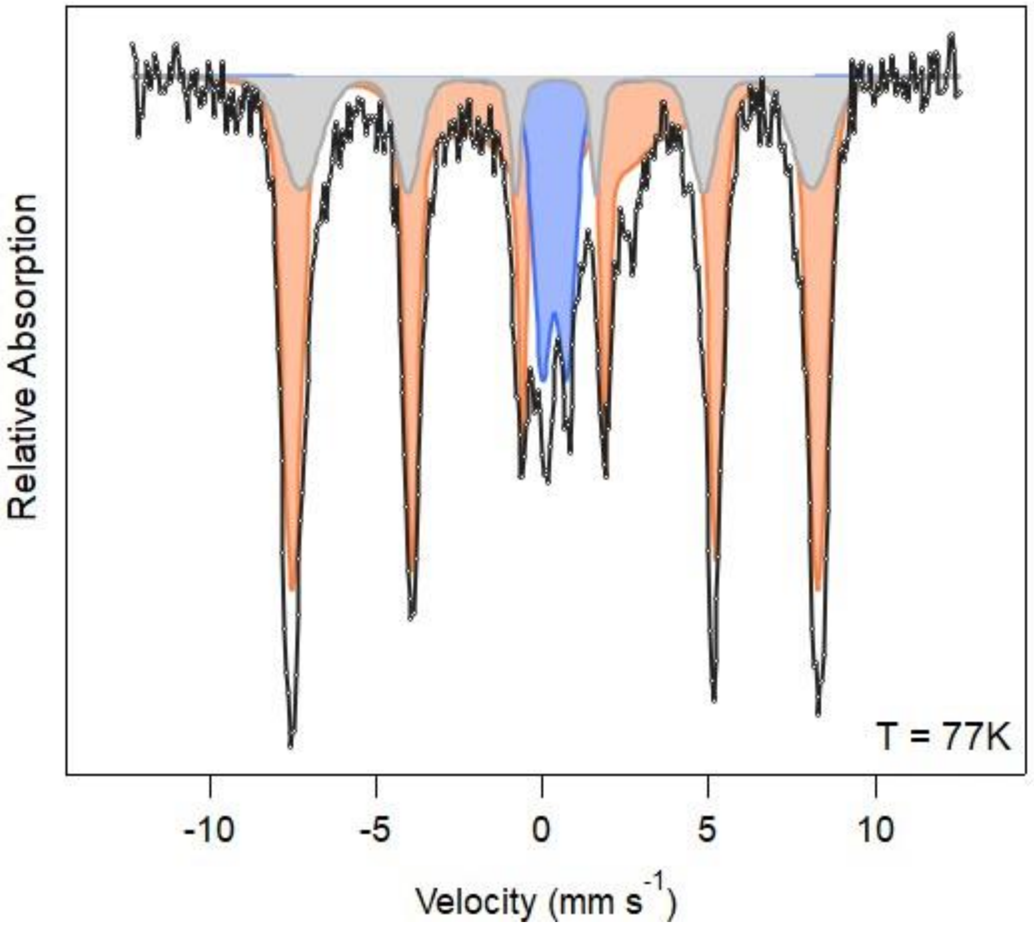

Figure S4. Mössbauer spectra of filtered aqueous Fe(II) solution after 2 weeks. Open circles represent data points and lines connect adjacent data points for a visual aid. **Experimental conditions**: 0.1 mM NO_2^-, 1 mM ^{NA}Fe(II), 10 mM Sodium Bicarbonate buffer, initial pH 7.0.

Filtered aqueous solution:

The Mossbauer spectrum above indicates the presence of goethite, and lepidocrocite which is consistent with previous XRD, and EXAFs observations of goethite, two-line ferrihydrite, and lepidocrocite formation from aqueous Fe(II) oxidation by nitrite.[1] Our spectrum is relatively undefined likely because of limited amounts of Mossbauer active ^{57}Fe present in the filtered sample. It is likely that the remaining unfitted area could resemble another Fe mineral such as ferrihydrite, similar to what others have observed,[1] however, we were unable to adequately fit the area with parameters similar to ferrihydrite.

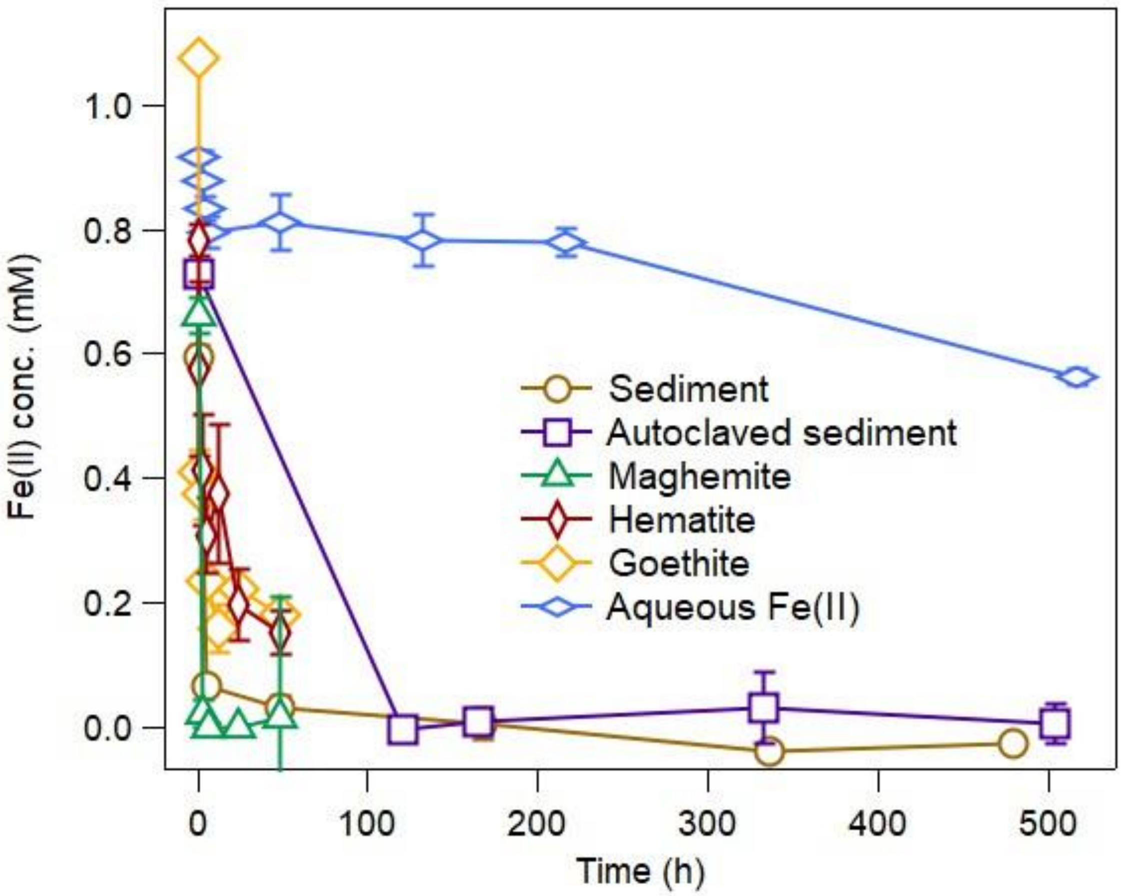

Figure S5. Aqueous Fe(II) concentration over time in each of the Fe environments investigated for NO_2^- reduction. Experimental conditions: 5 g/L Fe oxide or 10 g/L sediment, 1 mM Fe(II), 0.1 mM NO_2^-, 10 mM $NaHCO_3$, initial pH 7.0

Sorbed Fe(II):

To calculate the amount of Fe(II) sorbed onto Fe minerals we took the difference between the initial Fe(II) measurement and the first Fe(II) measurement conducted after the initial.

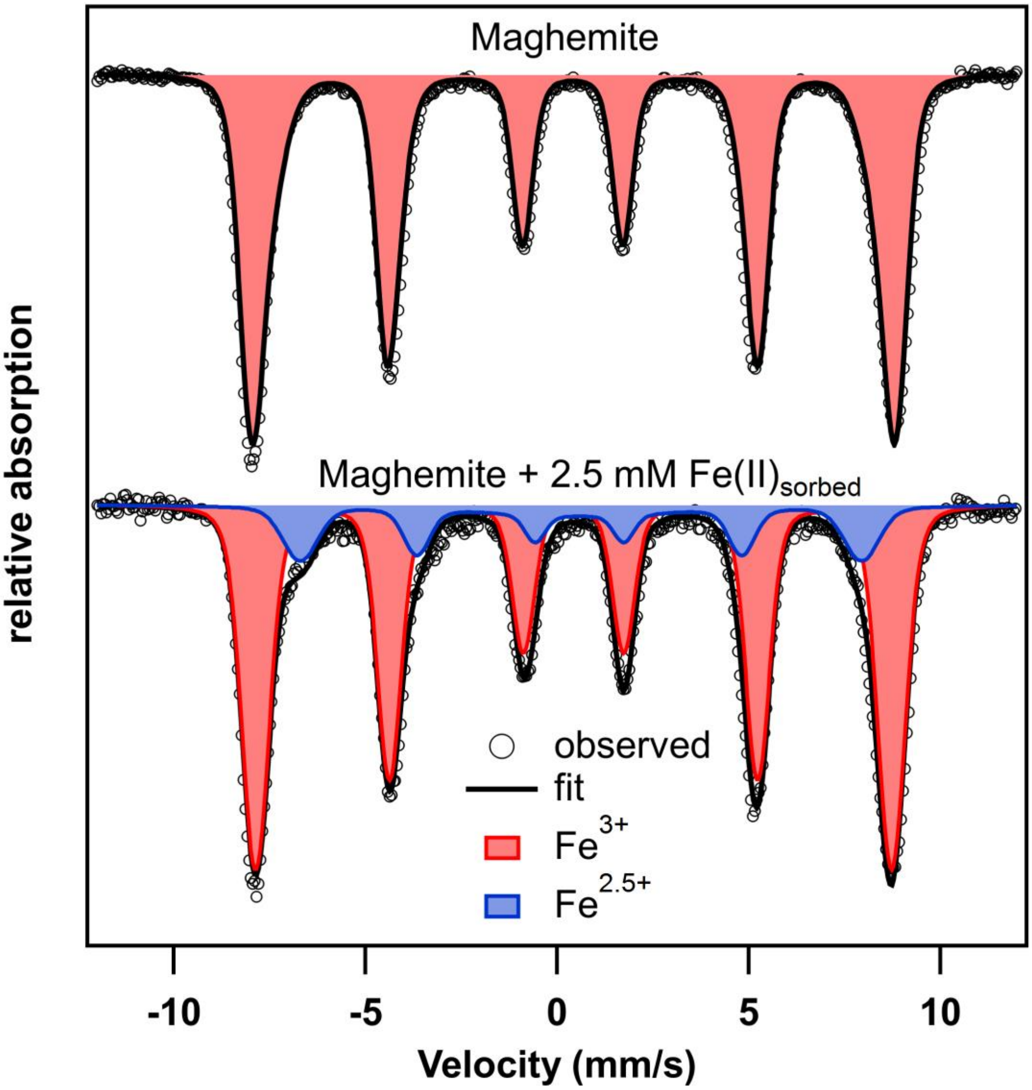

Figure S6. Maghemite before (top) and after reaction (bottom) with 7.7 mM ^{NA}Fe(II), showing that electron transfer occurs between Fe(II) and maghemite. Conditions: 1 g/L maghemite, 7.7 mM ^{NA}Fe(II) pH 7.2, 25 mM MOPS/NaCl buffer, x_{MB} = 0.13, x calculated from sorption = 0.20. Reaction time = 3.75 h.

Table S1. Mössbauer fitting parameters for spectra pictured in Figure S2

Sample name (χ^2)	CS[a] (mm/s)	QS[b] (mm/s)	H[c] (T)	Area (%)
Walnut Creek Alone 16K				
Fe(II) doublet	1.32	2.68	-	5.0
Fe(III) doublet	0.49	0.65	-	63.1
Fe(III) sextet	0.48	-0.12	46.83	31.9
Walnut Creek Autoclaved 16K				
Fe(II) doublet	1.28	2.66	-	4.4
Fe(III) doublet	0.48	0.65	-	56.0
Fe(III) sextet	0.48	-0.11	46.95	39.6

[a] Center shift relative to α-Fe(0).

[b] Quadrupole splitting.

[c] Hyperfine splitting

Table S2. Reported rates of NO_2^- reduction and extents of N_2O production in the literature.

Fe Environment	*k* (units vary)	Half life (h)	Nitrogen recovery (%)	pH	Aq. Fe(II) (mM)	NO_2^- (mM)	Solids loading (g L^{-1})	Reference
Aqueous Fe(II)	2.35×10^{-2} h^{-1}	29.5	40	7	10	10	0	Jones, 2015
	4.00×10^{-3} h^{-1}	173.3	2	5.5	9.3	3	0	Chen, 2020
	8.00×10^{-3} h^{-1}	86.6	4	6	9.3	3	0	
	2.70×10^{-2} h^{-1}	25.7	5	6.5	9.3	3	0	
	5.80×10^{-2} h^{-1}	12.0	5	7	9.3	3	0	
	7.00×10^{-4} h^{-1}	990.2	52[a]	7	0.6	0.2	0	Buchwald, 2016
	2.00×10^{-2} h^{-1}	34.7	52[a]	7	4.7	0.2	0	
	1.00×10^{-1} h^{-1}	6.9	52[a]	7	8.7	0.2	0	
	3.00×10^{-2} h^{-1}	23.1	52[a]	8	0.6	0.2	0	
	2.30×10^{-1} h^{-1}	3.0	52[a]	8	4.2	0.2	0	
	3.50×10^{-1} h^{-1}	2.0	52[a]	8	6.3	0.2	0	
	0 h^{-1}	0	-[b]	6.5	0.8	0.213	0	Grabb, 2016
	1.6×10^{-3} h^{-1}	433.2	0.0056	6.5	12	0.183	0	
	0.4 mol L^{-1} h^{-1}	750.0	4.2	7	-	0.1	0	Dhakal, 2021
	-	-	100	6.6	10	43	0	Kampschreur, 2011
	8.47×10^{-2} h^{-1}	8.2	90[c]	6.4	5	1.54	0	Margalef-Marti, 2020
	0.06 mM^{-1} d^{-1}	625.8	-	8.2	1	0.65	0	Fernandez, 2020
Goethite	4.60×10^{-1} h^{-1}	1.5	57	7	1	0.1	5	*This study*
Goethite	5.00×10^{-3} h^{-1}	138.6	52[a]	7	0.8	0.2	0.02	Buchwald, 2016
	1.50×10^{-1} h^{-1}	4.6	52[a]	7	4.8	0.2	0.08	
	2.90×10^{-1} h^{-1}	2.4	52[a]	7	7.9	0.2	0.08	
	5.00×10^{-2} h^{-1}	13.9	52[a]	8	1	0.2	0.02	
	6.90×10^{-1} h^{-1}	1.0	52[a]	8	4.5	0.2	0.08	
	1.68 h^{-1}	0.4	52[a]	8	8.1	0.2	0.08	
Goethite	1.33×10^{-1} h^{-1}	5.2	40[d]	7	10	10	-	Jones, 2015
Goethite	0.26 mol L^{-1} h^{-1}	1176.5	0.4	5.5	0	0.1	2	Dhakal, 2021
	0.28 mol L^{-1} h^{-1}	238.1	-	5.5	0	0.45	2	
	0.28 mol L^{-1} h^{-1}	116.5	-	5.5	0	0.92	2	
	0.11 mol L^{-1} h^{-1}	2727.3	-	5.5	0.07	0.1	2	
	0.11 mol L^{-1} h^{-1}	2727.3	-	5.5	0.42	0.1	2	
	0.72 mol L^{-1} h^{-1}	416.7	7	5.5	1.3	0.1	2	
Hematite	3.60×10^{-1} h^{-1}	2	58	7	1	0.1	5	*This Study*
x = 0.47	2.80×10^{-1} h^{-1}	2.5	30	7	1	0.1	5	*This Study*
x = 0.21	8.60×10^{-2} h^{-1}	8.2	21	7	1	0.1	5	
x = 0.41	5.40×10^{-2} h^{-1}	12.9	23	7	1	0.1	5	
Maghemite	1.00×10^{-2} h^{-1}	69	70	7	1	0.1	5	
Magnetite	1.20×10^{-3} h^{-1}	577.6	n.a.[e]	5.5	0	0.5	10	Dhakal, 2013

	1.10×10^{-3} h^{-1}	630.1	n.a.[e]	6.5	0	0.5	10	
	6.00×10^{-4} h^{-1}	1155.2	n.a.[e]	7.5	0	0.5	10	
Magnetite	7.30×10^{-3} h^{-1}	95.0	n.a.[e]	4.1	5	1.54	5	Margalef-Marti, 2020
Walnut Creek	1.80×10^{-3} h^{-1}	385.1	100	7	1	0.1	10	*This Study*
Montmorrilonite	2.00×10^{-4} h^{-1}	3465.7	31[f]	6.5	0.8	0.118	2.2	Grabb, 2016
	-	-	-	6.5	0	0.121	2.2	
Nontronite	8.00×10^{-3} h^{-1}	86.6	31[f]	6.5	1.3	0.1	18.1	
	3.00×10^{-3} h^{-1}	231.0	-	6.5	0	0.13	18.1	
Illite	1.00×10^{-4} h^{-1}	6931.5	31[f]	6.5	0.7	0.176	0.4	
	-	-	-	6.5	0	0.172	0.4	
Paddy Soil	31.4 mg N kg^{-1} d^{-1}	-	43[g]	7	3.2 g Fe kg^{-1}	100 mg N kg^{-1}	100	Wang, 2020
Ocean sediment	-	-	-	7.2	2	4	-	Otte, 2019
Kaolinite	-[h]	-	50	6.45	0.1	0.5	10	Rakshit, 2016
Siderite	0.22 M^{-1} h^{-1}	988.1	-	6.5	0	4.6	10	Rakshit, 2008
Lepidocrocite	0 h^{-1}	-	-	8	0.2	0.2	0.24	Sorensen, 1991
HFO	0.001 uM h^{-1}	3.7	-	6.8	0.262	0.717	2.5 mM	Tai and Dempsey, 2009
Ferrihydrite	0.22 mM^{-1} d^{-1}	143.5	-	8.2	0	0.76	10	Fernandez, 2020
	0.74 mM^{-1} d^{-1}	42.7	-	8.2	1.2	0.76	10	
Siderite	2.45×10^{-1} h^{-1}	2.83	n.a.[e]	4	5	1.1	5	Margalef-Marti, 2020
Olivine	7.73×10^{-2}	8.97	n.a.[e]	4.4	5	1.54	5	
Green Rusts (Chloride)	4.13 h^{-1}	0.17	31.3	6.5	1.3	0.1	4.7[i]	Grabb, 2016
	0.76 h^{-1}	0.91	7.2	6.5	0.4	0.191	1.3[i]	
	3.08 h^{-1}	0.23	28.5	6.5	0.7	0.101	4.2[i]	
	3.06 h^{-1}	0.23	16.5	6.5	1.1	0.185	3.5[i]	
	1.07 h^{-1}	0.65	9.5	6.5	0.3	0.197	1.4[i]	
	1.03 h^{-1}	0.67	-	6.5	0.9	0.168	1.1[i]	
	1.27 h^{-1}	0.55	-	6.5	1.1	0.187	1.2[i]	
	1.28 h^{-1}	0.54	8.7	6.5	0.9	0.213	1.4[i]	
	1.15 h^{-1}	0.60	-	6.5	1.1	0.179	1.6[i]	
	1.57 h^{-1}	0.44	9.9	6.5	0.4	0.206	2.7[i]	
	6.28 h^{-1}	0.11	-	6.5	2.3	0.964	4.9[i]	
	6.30 h^{-1}	0.11	-	6.5	1.1	0.934	5.0[i]	
	6.30 h^{-1}	0.11	-	6.5	1.5	0.18	5.3[i]	
	6.43 h^{-1}	0.11	-	6.5	1	0.219	5.6[i]	

Footnotes:

[a] N_2O recoveries ranged from 11 to 52%. Here we list the maximum noted percentage of 52%

[b] Dashed lines signify that data was not reported.

[c] Margalef Marti 90% vs. 0 %

[d] N_2O recoveries were reported to range from 15 to 40%. Here we list the maximum noted percentage of 40%.

[e] N_2O recoveries were reported as very low and have been noted as not applicable.

[f] N_2O recoveries were reported to range from 7 to 31%. Here we list the maximum noted percentage of 31%.

[g] N_2O recoveries between the two reported sediments (S1 and S2) were listed as 20.5 and 42.9% respectively. Here we list the maximum noted percentage of 43%

[h] No rates were reported for the two experiments conducted with high and low concentrations of Fe(II), however, it was noted that in the experiment with higher Fe(II) concentrations the rate was 2.4 times that of the lower Fe(II) experiment. Here we list the values reported for the high Fe(II) concentration experiment.

[i] Mass loadings for precipitated green rusts were calculated using the molar mass and the reported concentration of green rust in mM.

Maghemite stoichiometry change:

We estimated the degree to which the stoichiometry would change in our maghemite + Fe(II) experiment. We added 75 mg of Maghemite which has a molar mass of 159.69 g mol^{-1}. From our solids we measured 0.47 mmol of Fe(III) present. We then observed the sorption of approximately 0.661 ± 0.01 mM Fe(II) which was calculated from the initial Fe(II) measurement because by 24 hours no Fe(II) was detected in the aqueous solution of the experiment. If we assume a direct 1:1 electron transfer from the sorbed fe(II), we would expect to see a stoichiometry increase of 0.01 mmol Fe(II) / 0.47 mmol Fe(III) or $x = 0.02$.

Previous work by our group[2, 3] has demonstrated that electron transfer from aqueous Fe(II) to a non-stoichiometric magnetite results in an increase to magnetite stoichiometry, however, we are unaware of any work showing that Fe(II) also transfers electrons to maghemite converting it to non-stoichiometric magnetite. Therefore, we conducted an experiment to probe whether electron transfer between maghemite and Fe(II) occurs, but at a lower solids loading (1 g L^{-1} of ^{NA}maghemite) and higher Fe(II) concentration (7.7 mM ^{NA}Fe) where we could observe a greater increase in the magnetite stoichiometry. The sorption and reaction of Fe(II) with maghemite resulted in the appearance of a secondary sextet in the maghemite spectrum (**Figure S5**) with a center shift value consistent with that of an $^{oct}Fe^{2.x+}$ sextet (CS = 0.61 mm/s), but one that was not fully $Fe^{2.5+}$ with a CS = 0.72 mm/s . The newly formed sextet resulted in an magnetite x_{MB} value of 0.13, close to the expected value of 0.20 calculated from the sorption of Fe(II) (2.5 mM Fe(II) sorbed).

Fe(II) available in Walnut Creek sediment for NO_2^- reduction

To calculate the amount of Fe(II) available in Walnut Creek sediment for NO_2^- reduction, we used ^{57}Mössbauer spectroscopy and a 5M HCl extraction and found that there was enough Fe(II) present to reduce ~48% of the added NO_2^-.

We added 10 mL of 5M HCl to 150 mg of Walnut Creek sediment and allowed the sediment to extract overnight. We then sampled the extracted Fe using the 1,10 phenanthroline method and measured an Fe_{Tot} concentration in solution of 3.61 mM Fe. We also analyzed the solution using ICP-MS and similarly measured an Fe concentration of 3.76 mM Fe. From our 1,10 phenanthroline analysis we calculated that there was approximately 0.241 mmol of Fe per g of sediment. To calculate the Fe(II) present we estimated by taking the Fe(II) percent area (4%) of the Mössbauer spectra for autoclaved Walnut Creek sediment alone (**Figure S2**). The Mössbauer sample was made up by combining two separate reactors each with 150 mg into one sample meaning the total mass represented was approximately 300 mg which results in approximately 0.0723 mmol of Fe present in the total sample, or 2.892 µmol Fe(II) present. For each reactor bottle 1.5 µmol of NO_2^- was added for a total of 3.0 µmol of NO_2^- from the combined reactors. To calculate the percent of NO_2^- that could be reduced by the Fe(II) present in the sediment we use the ratio of 2 µmol of Fe(II) are required to reduce 1 µmol of NO_2^- to N_2O. Our result is that 48.2% of the added NO_2^- would be reduced by Fe(II) present in the sediment.

Additionally, we also calculated the total percent of Fe in the sediment mass which came to approximately 1.3% Fe present. We initially calculated that 2.02 mg Fe present were present in the sediment and in relation to the 150 mg of sediment used we calculated that 0.013 mg of Fe were present for each gram of sediment used.

Goethite and Hematite redox potential calculations

To compare the redox potentials of the goethite and hematite systems we approximated the potential (E_H) of each mineral in the presence of 1 mM Fe(II). First, we calculated the activity of Fe(II) at our conditions using, the extended form of the Debye-Hückel equation, which was 0.645. Now with the calculated Fe(II) concentration and the activity we were able to calculate the potential using the following equation:

$$E_H = E_H^0 - 0.059*\log(Fe^{2+})-0.177*pH$$

Where E_H^0 is the formal potential for goethite (800 mV vs. SHE) and hematite (739 mV vs. SHE) and the pH was 7.0. As for the Fe concentration we used the final Fe(II) concentration measurement for each experiment (0.18 mM Fe(II) for goethite, and 0.15 mM Fe(II) for hematite). From these calculations we arrive at the potential of -456 mV vs. SHE for goethite + Fe(II) and -451 mV vs. SHE for hematite + Fe(II).

References:

1. L. C. Jones, B. Peters, J. S. Lezama Pacheco, K. L. Casciotti and S. Fendorf, Stable Isotopes and Iron Oxide Mineral Products as Markers of Chemodenitrification, *Environmental Science & Technology*, 2015, **49**, 3444-3452.
2. C. A. Gorski and M. M. Scherer, Influence of Magnetite Stoichiometry on FeII Uptake and Nitrobenzene Reduction, *Environmental Science & Technology*, 2009, **43**, 3675-3680.
3. D. E. Latta, C. A. Gorski and M. M. Scherer, Influence of Fe(2+)-catalysed iron oxide recrystallization on metal cycling, *Biochem Soc Trans*, 2012, **40**, 1191-1197.